Inorganic Chemistry

Article

pubs.acs.org/IC

Positional Flexibility: Syntheses and Characterization of Six Uranium Chalcogenides Related to the 2H Hexagonal Perovskite Family

Adel Mesbah,[†,‡] Jai Prakash,[†] Jessica C. Beard,[†] Eric A. Pozzi,[†] Mariya S. Tarasenko,[†] Sébastien Lebègue,[§] Christos D. Malliakas,[†] Richard P. Van Duyne,[†] and James A. Ibers*[,†]

[†]Department of Chemistry, Northwestern University, 2145 Sheridan Road, Evanston, Illinois 60208-3113, United States

[‡]ICSM, UMR 5257 CEA/CNRS/UM2/ENSCM, Site de Marcoule, Bâtiment 426, BP 17171, 30207 Bagnols-sur-Cèze cedex, France

[§]Laboratoire de Cristallographie, Résonance Magnétique et Modélisations (CRM2, UMR CNRS 7036), Institut Jean Barriol, Université de Lorraine, Boulevard des Aiguillettes, BP 239, 54506 Vandoeuvre-lès-Nancy, France

Supporting Information

ABSTRACT: Six new uranium chalcogenides, Ba_4USe_6, Ba_3FeUSe_6, Ba_3MnUSe_6, Ba_3MnUS_6, $Ba_{3.3}Rb_{0.7}US_6$, and $Ba_{3.2}K_{0.8}US_6$, related to the 2H hexagonal perovskite family have been synthesized by solid-state methods at 1173 K. These isostructural compounds crystallize in the K_4CdCl_6 structure type in space group D_{3d}^6–$R\bar{3}c$ of the trigonal system with six formula units per cell. This structure type is remarkably flexible. The structures of Ba_3FeUSe_6, Ba_3MnUSe_6, and Ba_3MnUS_6 consist of infinite $^1_\infty[MUQ_6^{6-}]$ chains (M = Fe or Mn; Q = S or Se) oriented along the *c* axis that are separated by Ba atoms. These chains are composed of alternating M-centered octahedra and U-centered trigonal prisms sharing triangular faces; in contrast, in the structures of Ba_4USe_6, $Ba_{3.3}Rb_{0.7}US_6$, and $Ba_{3.2}K_{0.8}US_6$, there are U-centered octahedra alternating with Ba-, Rb-, or K-centered trigonal prisms. Moreover, the Ba_4USe_6, Ba_3FeUSe_6, Ba_3MnUSe_6, and Ba_3MnUS_6 compounds contain U^{4+}, whereas $Ba_{3.3}Rb_{0.7}US_6$ and $Ba_{3.2}K_{0.8}US_6$ are mixed $U^{4+/5+}$ compounds. Resistivity and μ-Raman spectroscopic measurements and DFT calculations provide additional insight into these interesting subtle structural variations.

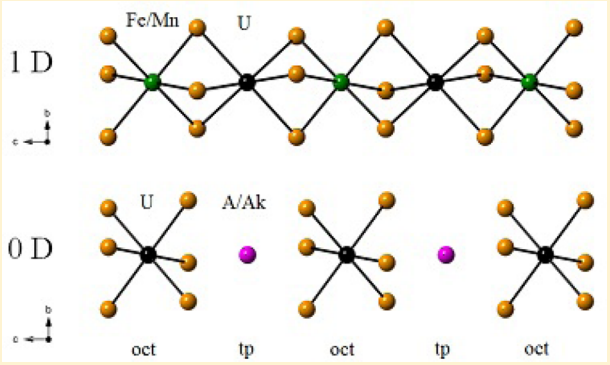

INTRODUCTION

Perovskites are among the most studied inorganic solid-state compounds as they show a variety of interesting physical properties, including intriguing magnetic behavior, superconductivity, thermoelectricity, and ionic conductivity.[1] The crystal structure of the prototype perovskite of formula ABO_3 has cubic symmetry and is three-dimensional.[2] Here, A and B are cations of very different sizes. The O atoms bond to both. The B atoms are octahedrally coordinated, and the A atoms are 12-fold coordinated in a cuboctahedron. From this cubic structure, there are numerous derivatives arising from diverse combinations of not only the cations but also the anions. Some differences in the sizes of the A and B elements lead to a change in the crystal system and stabilization of the hexagonal form. The resultant hexagonal structures range from three-dimensional to zero-dimensional salts. Among these are the 2H hexagonal perovskite-related structures that exhibit one-dimensional infinite chains separated in general by alkaline-earth elements.[3−5] These and other low-dimensional inorganic compounds are of particular interest as they exhibit a wide range of structures and physical properties.[6−12] A general formula for the 2H hexagonal perovskite-related compounds is[13] $A_{3n+3m}A'_nB_{3m+n}O_{9m+6n}$. The structure consists of stacking sequences of BO_6 octahedra and $A'O_6$ trigonal prisms, where n/m is the ratio between $[A_3A'O_6]$ and $[A_3O_9]$ layers. Here, A is usually an alkaline-earth element; B is the element filling the octahedral site, and A′ is the element positioned in the trigonal prism. A′ can be A, B, or another element; hence, these structures are highly flexible in their compositions. The oxides[5] and the halides are the most reported compounds in the perovskites family; however, there is increased interest in the chalcogenides. In fact, some of these have different applications, such as in photovoltaics.[14] Recently, 2H perovskite-related structures have been reported that contain f elements. These show different sequences in the arrangement of the BO_6 octahedra and the $A'O_6$ trigonal prisms. An example is the structure of $Ba_4Cr_2US_9$[15] with $n = 3$ and $m = 1$. Other examples are the few reported f-element structures of the K_4CdCl_6[16] structure type ($n = 1$, $m = 0$) in which there are infinite chains composed of the equal alternation of A′ trigonal prisms and B octahedra. These include $Ba_{3.69}US_6$,[17] Ba_3FeUS_6,[18] Ba_3AgUS_6,[18] and Ba_3LnInS_6 (Ln = Pr, Sm, Gd, Yb).[19]

Received: December 18, 2014
Published: February 20, 2015

DOI: 10.1021/ic5029806
Inorg. Chem. 2015, 54, 2851−2857

Table 1. Crystallographic Data and Structure Refinement Details for Six Uranium Chalcogenides[a]

	Ba_4USe_6	Ba_3FeUSe_6	Ba_3MnUSe_6	Ba_3MnUS_6	$Ba_{3.3}Rb_{0.7}US_6$	$Ba_{3.2}K_{0.8}US_6$
fw (g mol^{-1})	1261.15	1179.66	1178.75	897.35	927.88	881.51
a (Å)	12.5997(2)	12.4842(10)	12.4561(2)	12.0220(5)	12.0875(3)	12.0798(2)
c (Å)	15.6063(2)	13.9258(11)	14.1354(3)	13.6410(6)	15.1516(5)	15.0309(3)
V (Å^3)	2145.61(7)	1879.6(3)	1899.34(7)	1707.38(16)	1917.18(11)	1899.48(7)
ρ (g cm^{-3})	5.856	6.253	6.183	5.236	4.822	4.726
μ (mm^{-1})	37.349	40.668	40.097	26.519	26.458	23.752
$R(F)^b$	0.014	0.014	0.015	0.011	0.009	0.011
$R_w(F_o^2)^c$	0.030	0.028	0.029	0.023	0.019	0.019

[a]For all structures, space group D_{3d}^6–$R\bar{3}c$, λ = 0.71073 A, T = 100(2) K, and Z = 6. [b]$R(F) = \sum||F_o| - |F_c||/\sum|F_o|$ for $F_o^2 > 2\sigma(F_o^2)$. [c]$R_w(F_o^2) = \{\sum[w(F_o^2 - F_c^2)^2]/\sum wF_o^4\}^{1/2}$. For $F_o^2 < 0$, $w^{-1} = \sigma^2(F_o^2)$. For $F_o^2 \geq 0$, $w^{-1} = \sigma^2(F_o^2) + (qF_o^2)^2$, where q = 0.0132 for Ba_4USe_6, 0.0091 for Ba_3FeUSe_6, 0.0116 for Ba_3MnUSe_6, 0.0065 for Ba_3MnUS_6, 0.0066 for $Ba_{3.3}Rb_{0.7}US_6$, and 0.0043 for $Ba_{3.2}K_{0.8}US_6$.

In this present work, we present the syntheses and characterizations of six new uranium chalcogenides of the 2H hexagonal perovskite-related family that crystallize in the K_4CdCl_6 structure type (space group D_{3d}^6–$R\bar{3}c$). Their structures demonstrate remarkable flexibility in the position of the U atom in the structure and its resultant oxidation state. Characterization of these compounds includes μ-Raman and resistivity measurements and DFT calculations.

EXPERIMENTAL METHODS

Syntheses. The U powder was prepared by hydridization of depleted U turnings (IBI Laboratories) using a modified,[20] previously published procedure.[21] All other reactants were used as supplied: Ba (Johnson Matthey, 99.5%), Se (Cerac, 99.999%), S (Mallinckrodt, 99.6%), Mn (Johnson Matthey, 99.3%), Fe (Aesar, 99.99%), CsCl (Aldrich, 99.9%), RbCl (Alfa, 99.8%), and KCl (Aldrich, 99%+). The starting materials were loaded into 6 mm carbon-coated fused-silica tubes inside an Ar-filled drybox. They were then transferred, evacuated to 10^{-4} Torr, and flame-sealed. With the exception of Ba_4USe_6, the tubes were heated to 1173 K in 48 h, annealed there for 4 d, then cooled to 673 K at a rate of 2.5 K/h, then to 298 K in 12 h. Semiquantitative energy dispersive X-ray (EDX) spectroscopic analysis was carried out on selected single crystals from each reaction product with the use of a Hitachi S-3400 SEM microscope.

Synthesis of Ba_4USe_6. Black crystals of Ba_4USe_6 were obtained from the reaction of Ba (46.72 mg, 0.340 mmol), U (20.2 mg, 0.085 mmol), and Se (40.3 mg, 0.510 mmol) with CsCl flux (200 mg). The reaction tube was heated to 773 K in 12 h, held there for 12 h, ramped to 1173 K in 24 h, and annealed for 96 h. The tube was then cooled to 673 K in 48 h and finally to 298 K in 12 h. The reaction product contained black needles and plates of Ba_4USe_6 and crystals of U_3Se_4.[22] The black needles and plates showed U:Ba:Se ≈ 1:4:6.

Synthesis of Ba_3FeUSe_6. Black crystals of Ba_3FeUSe_6 were obtained from the reaction of Ba (35 mg, 0.255 mmol), Fe (4.7 mg, 0.085 mmol), U (20.2 mg, 0.085 mmol), and Se (40.1 mg, 0.51 mmol) in 100 mg of CsCl used as flux. Three products were found: black crystals of Ba_3FeUSe_6 showing Ba:Fe:U:Se ≈ 3:1:1:6, black blocks of a possible new quaternary with the composition Ba:Fe:Se:Cl ≈ 6:2:11:1, and UOSe.[23]

Synthesis of Ba_3MnUSe_6. Black crystals of Ba_3MnUSe_6 were obtained by the reaction of Ba (35 mg, 0.255 mmol), Mn (4.7 mg, 0.085 mmol), U (20.2 mg, 0.085 mmol), and Se (40.1 mg, 0.51 mmol) in CsCl (50 mg) used as flux. Three different compounds were found: black blocks of Ba_3MnUSe_6 showing Ba:Mn:U:Se ≈ 3:1:1:6, square plates of UOSe, and orange plates of Ba_2MnSe_3.[24]

Synthesis of Ba_3MnUS_6. Small black plates of Ba_3MnUS_6 were obtained in a direct combination of Ba (35 mg, 0.255 mmol), Mn (4.66 mg, 0.085 mmol), U (20 mg, 0.085 mmol), and S (16 mg, 0.51 mmol). Found was Ba:Mn:U:S ≈ 3:1:1:6 with UOS as a byproduct.

Synthesis of $Ba_{3.3}Rb_{0.7}US_6$. The reaction of Ba (35 mg, 0.255 mmol), U (20 mg, 0.085 mmol), and S (16 mg, 0.51 mmol) in 100 mg of RbCl flux produced black crystals of $Ba_{3.3}Rb_{0.7}US_6$, showing Ba:Rb:U:S ≈ 3.3:0.7:1:6 as well as UOS and an excess of RbCl.

Synthesis of $Ba_{3.2}K_{0.8}US_6$. The reaction of Ba (35 mg, 0.255 mmol), U (20 mg, 0.085 mmol), S (16 mg, 0.51 mmol) in a KCl flux (50 mg) produced small black plates of $Ba_{3.2}K_{0.8}US_6$, showing Ba:K:U:S ≈ 3.2:0.8:1:6 as well as UOS.

Structure Determinations. The crystal structures of the six compounds, Ba_4USe_6, Ba_3FeUSe_6, Ba_3MnUSe_6, Ba_3MnUS_6, $Ba_{3.3}Rb_{0.7}US_6$, and $Ba_{3.2}K_{0.8}US_6$, were determined from single-crystal X-ray diffraction data collected with the use of graphite-monochromatized Mo Kα radiation (λ = 0.71073 A) at 100(2) K on a Bruker APEX2 diffractometer.[25] The algorithm COSMO implemented in the program APEX2 was used to establish the data collection strategy with a series of 0.3° scans in ω and φ. The exposure time was 10 s/frame, and the crystal-to-detector distance was 60 mm. The collection of intensity data as well as cell refinement and data reduction were carried out with the use of the program APEX2.[25] Face-indexed absorption, incident beam, and decay corrections were performed with the use of the program SADABS.[26] All the structures were solved and refined with the SHELX14 program package.[26,27] The structure refinements of Ba_4USe_6, Ba_3FeUSe_6, Ba_3MnUSe_6, and Ba_3MnUS_6 were straightforward. However, those for $Ba_{3.3}Rb_{0.7}US_6$ and $Ba_{3.2}K_{0.8}US_6$ were not. The best solution for each of these structures involved placing at the crystallographic site 32 the composition (Ba/Rb or Ba/K) dictated by the EDX results. The program STRUCTURE TIDY[28] in PLATON[29] was used to standardize the atomic positions. Further details are given in Table 1 and in the Supporting Information.

μ-Raman Spectroscopy. Raman spectroscopy was performed using a Nikon Eclipse Ti2000-U inverted microscope in a manner similar to that previously described.[30] A stabilized 785 nm diode laser (Innovative Photonic Solutions) was aligned into the microscope through a 50× extra-long working distance objective (numerical aperture = 0.55), which focused the incident beam onto #2 glass coverslips supporting the synthesized single crystal. The same objective collected the scattered light, which was then focused onto the 100 μm entrance slit of an Acton SP2300 imaging spectrometer. A 150 groove/mm grating dispersed the collected light onto a liquid N_2-cooled, back-illuminated CCD (Spec10:400BR, Princeton Instruments). Crystals were irradiated with 830 μW, except for weakly scattering Ba_3MnUS_6 for which 6.8 mW was used. All spectra were collected for 10 s.

Resistivity Studies. Four-probe temperature-dependent resistivity data were collected using a homemade resistivity apparatus equipped with a Keithley 2182 nanovoltmeter, a Keithley 236 source-measure unit, and a high-temperature vacuum chamber controlled by a K-20 MMR system. An I–V curve from 1×10^{-5} to -1×10^{-5} A with a step of 2×10^{-6} A was measured for each temperature point, and resistance was calculated from the slope of the I–V plot. Data acquisition was controlled by custom-written software. Graphite paint (PELCO isopropanol-based graphite paint) was used for electrical contacts with Cu of 0.025 mm thickness (Omega). Direct current was applied along an arbitrary direction.

DOI: 10.1021/ic5029806
Inorg. Chem. 2015, 54, 2851−2857

Table 2. Interatomic Distances (Å)[a] in the Present and Related Compounds

distance (Å)	Ba_4USe_6	Ba_3FeUSe_6	Ba_3MnUSe_6	Ba_3MnUS_6	$Ba_{3.3}Rb_{0.7}US_6$[d]	$Ba_{3.2}K_{0.8}US_6$[d]	Ba_3FeUS_6[e]	Ba_3AgUS_6[e]	$Ba_{3.69}US_6$[f]
U1−Se1 × 6	2.825(1)[c]	2.836(1)[b]	2.842(1)[b]	2.724(1)[b]	2.655(1)[c]	2.635(1)[c]	2.712(1)[b]	2.609(1)[c]	2.658(1)[c]
M1−Se1 × 6	3.221(1)[b]	2.676(1)[c]	2.721(1)[c]	2.607(1)[c]	3.139(1)[b]	3.115(1)[b]	2.554(1)[c]	2.880(1)[b]	3.079(1)[b]
Ba1−Se1 × 2	3.348(1)	3.274(1)	3.261(1)	3.132(1)	3.242(1)	3.231(1)	3.141(1)	3.149(1)	3.128(1)
Ba1−Se1 × 2	3.384(1)	3.282(1)	3.332(1)	3.237(1)	3.250(1)	3.241(1)	3.175(1)	2.192(1)	3.240(1)
Ba1−Se1 × 2	3.413(1)	3.387(1)	3.397(1)	3.287(1)	3.264(1)	3.262(1)	3.273(1)	3.303(1)	3.280(1)
Ba1−Se1 × 2	3.513(1)	3.417(1)	3.399(1)	3.294(1)	3.409(1)	3.407(1)	3.305(3)	3.385(1)	3.404(1)

[a]All distances have been rounded from CIF files in the Supporting Information to facilitate comparisons. [b]Symmetry site 32 (trigonal prism). [c]Symmetry site $\bar{3}$. (octahedral). [d]Both Ba and the alkali metal are placed at the same site (trigonal prism). [e]From ref 18. [f]From ref 17.

DFT Calculations. Ab initio calculations were performed with the Vienna ab initio simulation package (VASP)[31,32] using the Heyd, Scuseria, Ernzerhof (HSE)[33−36] functional within density functional theory[37,38] and the projector augmented wave method.[39] Spin polarization was allowed. The cell and atom positions were taken identical to the experimental values. For a given compound, the various magnetic orders allowed in a crystallographic cell were calculated, and the one with the lowest total energy was retained as the ground state configuration. The default cutoff for the plane-wave part of the wave function and a *k*-point mesh of 4 × 4 × 4 to sample the Brillouin zone were used to reach numerical convergence.

RESULTS

Syntheses. The six compounds, Ba_4USe_6, Ba_3FeUSe_6, Ba_3MnUSe_6, Ba_3MnUS_6, $Ba_{3.3}Rb_{0.7}US_6$, and $Ba_{3.2}K_{0.8}US_6$, were obtained in >50 wt % yields by the reactions of the elements at 1173 K. The synthesis of Ba_3MnUSe_6 did not involve a flux, whereas the syntheses of the other compounds involved an alkali-metal chloride as a flux. Inability to separate these compounds from diverse byproducts, including UOS and UOSe, severely limits useful information that might have been obtained from magnetic studies. Regrettably, the actinide chalcogenides are highly oxyphilic and usually the products of our reactions are accompanied by UOQ phases that result from the etching of the carbon-coated fused-silica tubes. In some instances, interesting but surprising new O-containing compounds have resulted.[40,41]

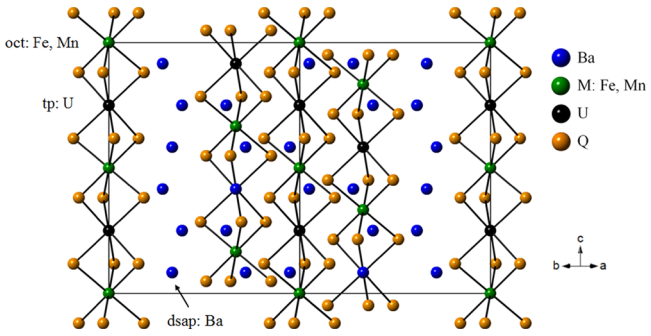

Figure 1. General view of the structure of Ba_3FeUSe_6, Ba_3MnUSe_6, and Ba_3MnUS_6 along [110]. Oct, tp, and dsap are abbreviations for octahedron, trigonal prism, and distorted square antiprism, respectively.

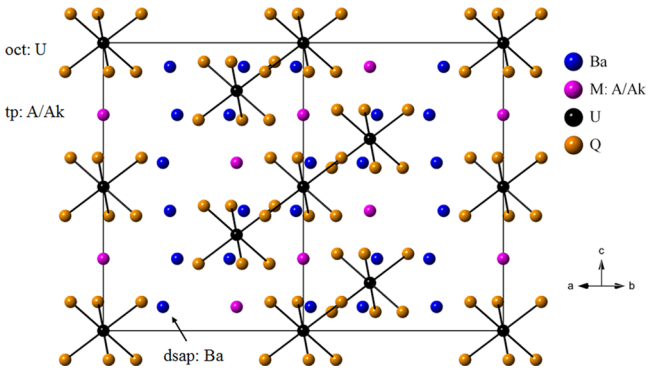

Figure 2. A view of the structure of Ba_4USe_6, $Ba_{3.3}Rb_{0.7}US_6$, and $Ba_{3.2}K_{0.8}US_6$ along [110]. Here, A = Rb or K, and Ak = Ba. Oct, tp, and dsap are abbreviations for octahedron, trigonal prism, and distorted square antiprism, respectively.

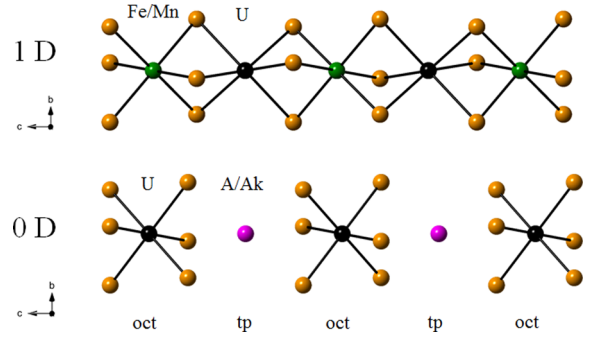

Figure 3. Infinite chains along the *c* axis in the Ba_3MUQ_6 family showing the evolution of structure dimensionality; oct and tp correspond to octahedra and trigonal prism, respectively.

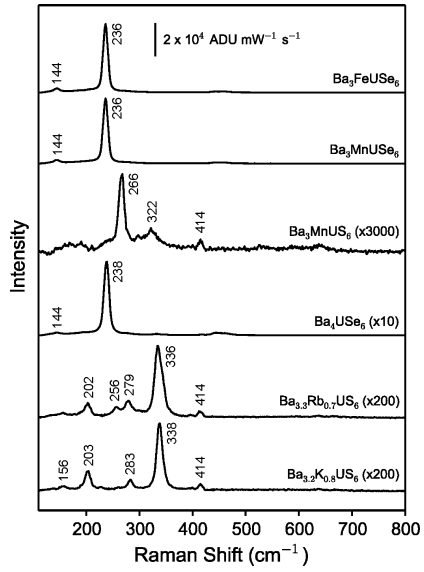

Figure 4. Raman spectra of the synthesized compounds using 785 nm excitation. U−S/Se stretches are observed for U in trigonal prismatic coordination (upper three spectra) and in octahedral coordination (lower three spectra).

DOI: 10.1021/ic5029806
Inorg. Chem. 2015, 54, 2851−2857

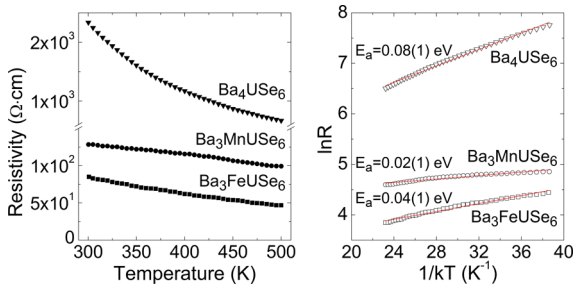

Figure 5. Resistivity and the corresponding Arrhenius plots for Ba_4USe_6, Ba_3FeUSe_6, and Ba_3MnUSe_6.

Crystal Structures. The compounds Ba_4USe_6, Ba_3FeUSe_6, Ba_3MnUSe_6, Ba_3MnUS_6, $Ba_{3.3}Rb_{0.7}US_6$, and $Ba_{3.2}K_{0.8}US_6$ are isostructural and crystallize in the K_4CdCl_6 structure type[16] in space group D_{3d}^6–$R\bar{3}c$ of the trigonal system with six formula units per cell (Table 1). Selected metrical data are reported in Table 2. Although the six compounds are isostructural in the classic sense,[28] their structures differ in the distribution of the atoms between the 32 and $\bar{3}$. sites.

Ba_3FeUSe_6, Ba_3MnUSe_6, and Ba_3MnUS_6. These structures have the same arrangement of atoms as in Ba_3FeUS_6.[18] The asymmetric unit comprises one U atom (site symmetry 32), one M (Fe or Mn) atom ($\bar{3}$.), one Ba atom (.2), and one Q (Se or S) atom (1). A general view of the structure is projected along [110] in Figure 1. In these three compounds, the U atom is connected to six Q atoms to form a trigonal prism, and the 3d element M is octahedrally coordinated to six Q atoms.

Ba_4USe_6, $Ba_{3.3}Rb_{0.7}US_6$, and $Ba_{3.2}K_{0.8}US_6$. These three compounds have the same arrangement of atoms as those in $Ba_{3.69}US_6$[17] and Ba_3AgUS_6[18] with the U atom in the $\bar{3}$. symmetry site (Figures 2 and 3). Consequently, the other site with 32 symmetry is filled by 1 Ba, 0.3 Ba + 0.7 Rb, and 0.2 Ba + 0.8 K for Ba_4USe_6, $Ba_{3.3}Rb_{0.7}US_6$, and $Ba_{3.2}K_{0.8}US_6$, respectively. In these three compounds, the U atom is octahedrally coordinated, and the Ba or mixed Ba/A site is trigonal-prismatically coordinated.

As detailed above, the six compounds belong to the 2H hexagonal perovskite-related family of general formula $A_{3n+3m}A'_nB_{3m+n}O_{9m+6n}$ with $n = 1$ and $m = 0$ as well as the previously published compounds $Ba_{3.69}US_6$, Ba_3FeUS_6, and Ba_3AgUS_6. The general observation[42] that insertion of an alkali metal into a metal chalcogenide lowers the dimensionality of the resultant structure also applies here for the insertion of an alkali-earth metal. The compounds Ba_3FeUSe_6, Ba_3MnUSe_6, and Ba_3MnUS_6 may be considered to have a one-dimensional structure with infinite $^1_\infty[MUQ_6^{6-}]$ chains formed by the alternation of the UQ_6 triangular prisms and MQ_6 octahedra through the sharing of triangular faces along the *c* axis. In contrast, the compounds Ba_4USe_6, $Ba_{3.3}Rb_{0.7}US_6$, and $Ba_{3.2}K_{0.8}US_6$ have a zero-dimensional structure formed by the alternation of isolated UQ_6 octahedra and MQ_6 (M = Ba or mixed Ba/A, A = Rb or K) trigonal prisms.

In all of these structures, the $^1_\infty[MUQ_6^{6-}]$ infinite chains are separated by Ba atoms (.2 symmetry site) as viewed in Figures 1 and 2. Each Ba atom is surrounded by a distorted square antiprism of eight Q (S, Se) atoms. The interatomic Ba–Q distances (Table 2) are typical.

Oxidation State and Structure Flexibility. In the Ba_4USe_6, Ba_3FeUSe_6, and Ba_3MnUSe_6 compounds, the U–Se distances are 2.8248(3), 2.8362(3), and 2.8422(3) Å, respectively. These compare favorably with those in the structures of the other six-coordinate U^{4+} compounds, for example, $Rb_2Pd_3USe_6$,[43] 2.8331(5) to 2.8659(7) Å; $RbAuUSe_3$,[44] 2.846(3) to 2.866(2) Å; and $CsAuUSe_3$,[44] 2.863(1) to 2.893(2) Å. In the Ba_3FeUSe_6 structure, the Fe–Se distance of 2.6761(3) Å may be compared with those of 2.4968(7) to 2.6782(7) Å for the $Fe^{2+}Se_6$ octahedra in $FeUSe_3$.[45] In the Ba_3MnUSe_6 structure, the Mn–Se distance is 2.7212(3) Å, which is between those of 2.696(1) to 2.736(1) Å for the Mn^{2+}–Se distance in the structure of Mn_2GeSe_4.[46] In the Ba_3MnUS_6 structure, the U–S distance of 2.7241(6) Å is typical for structures of 3d six-coordinate U^{4+} compounds, for example, 2.712(1) Å in the structure of Ba_3FeUS_6.[18] The Mn–S distance of 2.6067(2) Å is in agreement with Mn^{2+} in octahedral coordination as found in the Mn_2SnS_4 structure (2.604(1) to 2.620(2) Å).[47] There are no Q–Q bonds in these structures. Thus, the compounds Ba_4USe_6, Ba_3FeUSe_6, Ba_3MnUSe_6, and Ba_3MnUS_6 contain U^{4+} and M^{2+} and are charge balanced.

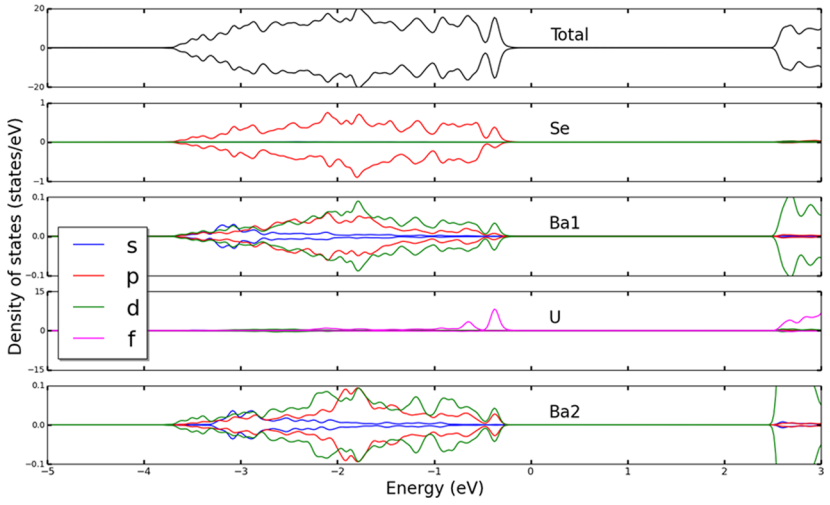

Figure 6. Total (upper plot) and partial density of states (PDOS, lower plots) of Ba_4USe_6. For each atom, the PDOS is projected onto the relevant orbitals.

DOI: 10.1021/ic5029806
Inorg. Chem. 2015, 54, 2851–2857

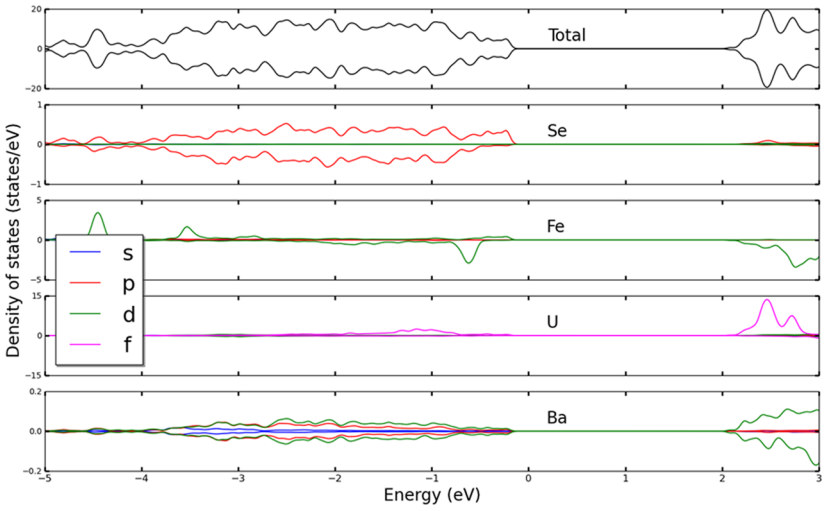

Figure 7. Total (upper plot) and partial density of states (PDOS, lower plots) of Ba_3FeUSe_6. For each atom, the PDOS is projected onto the relevant orbitals.

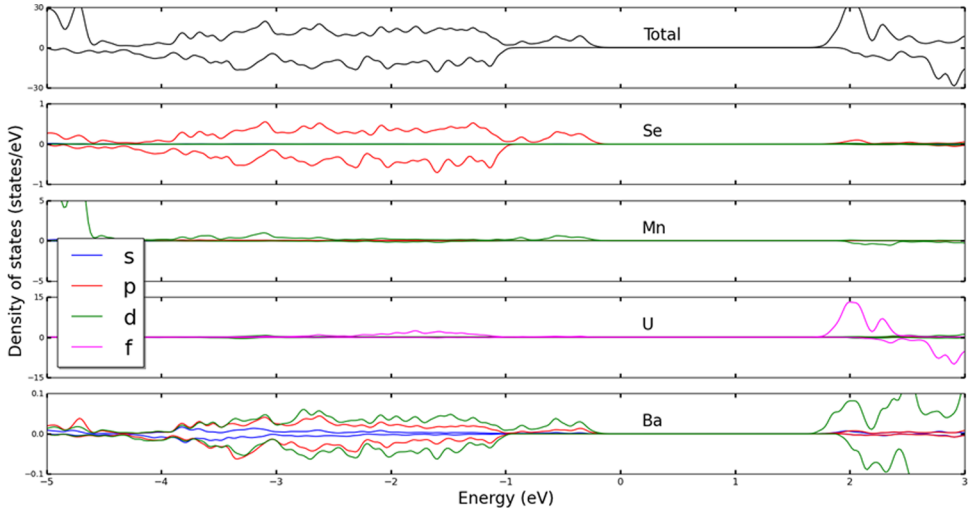

Figure 8. Total (upper plot) and partial density of states (PDOS, lower plots) of Ba_3MnUSe_6. For each atom, the PDOS is projected onto the relevant orbitals.

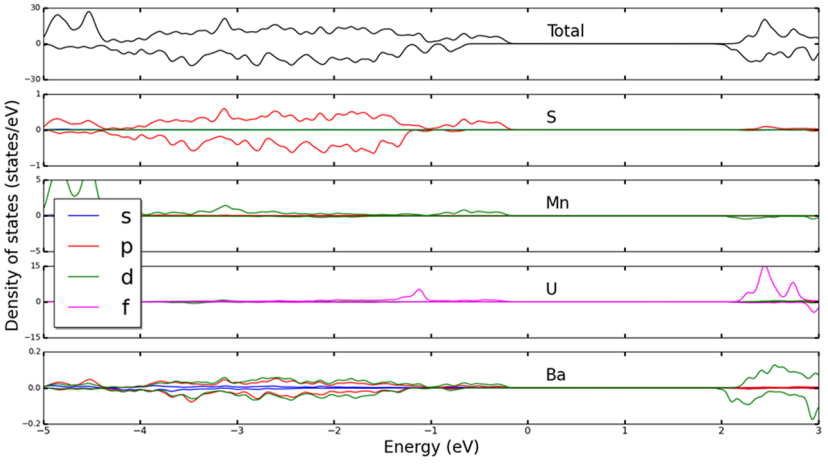

Figure 9. Total (upper plot) and partial density of states (PDOS, lower plots) of Ba_3MnUS_6. For each atom, the PDOS is projected onto the relevant orbitals.

The compounds $Ba_{3.3}Rb_{0.7}US_6$ and $Ba_{3.2}K_{0.8}US_6$ contain Ba^{2+}, Rb^+ or K^+, and S^{2-}. For charge balance of these two formulas, the average oxidation state of the U atoms must be +4.7 and +4.8, respectively. Thus, both of these compounds contain both

DOI: 10.1021/ic5029806
Inorg. Chem. 2015, 54, 2851−2857

U^{4+} and U^{5+} atoms in their structures. Indeed, the U−S distances of 2.655(1) and 2.636(1) Å compare well with that of 2.658(1) Å in $Ba_{3.69}US_6$,[17] another mixed U^{4+}/U^{5+} compound. Note that all of these distances, as expected, are shorter than typical U^{4+}−S distances.

As mentioned, the uranium chalcogenides crystallizing in the K_4CdCl_6 structure type display very interesting chemical flexibility in the position of the U atom (Figure 3). The tabulation in Table 2 indicates that this flexibility is driven by the nature of the second cation B or A′. Thus, the 3d elements Fe and Mn prefer octahedral coordination, and the flexible U atom goes to the A′ position (trigonal prismatic). However, the larger atoms (Ag, Ba, K, and Rb) clearly prefer the A′ site such that the flexible U atom goes to the B position (octahedral coordination).

This family of compounds presents a rare example of the chemical and positional flexibility that U can display in inorganic materials. In principle, we can tune the oxidation state of the U atoms by judicious choice of the relative sizes of the A′ and B atoms in the 2H perovskite-related compounds. An interesting challenge is to stabilize this structure with U^{3+} by adding a trivalent element, such as Al, Sc, Y, or even a lanthanide (Ln), but the latter could readily produce a disordered Ln/U structure.

Spectroscopic Properties. Raman spectra of the six synthesized compounds provide additional insight into their structures (Figure 4). Spectra of the one-dimensional structures Ba_3FeUSe_6, Ba_3MnUSe_6, and Ba_3MnUS_6 each exhibit a dominant low-wavenumber mode, likely owing to U−S/Se stretches within the trigonal prism. Both the Se-containing compounds exhibit this mode at 236 cm^{-1}, an unsurprising agreement given the similarity in U−Se interatomic distances in these compounds (Table 2). This mode is observed at 266 cm^{-1} for Ba_3MnUS_6. Symmetric U−S/Se stretching modes are observed at 336 and 338 cm^{-1} for $Ba_{3.3}Rb_{0.7}US_6$ and $Ba_{3.2}K_{0.8}US_6$, which are comparable with a previously reported U−S symmetric mode.[48] Whereas $Ba_{3.3}Rb_{0.7}US_6$ and $Ba_{3.2}K_{0.8}US_6$ contain identical U octahedra, the higher stretching frequency in $Ba_{3.2}K_{0.8}US_6$ is a result of shorter and stronger U−S interatomic distances in accordance with Badger's rule.[49] This mode is observed to lie substantially lower in frequency at 238 cm^{-1} for Ba_4USe_6 compared with that of its S analogues, consistent with the ∼0.2 Å increase in the U−S/Se interatomic distance and the greater mass of Se. Appreciably higher signal intensities observed in spectra of the Se-containing compounds cannot be explained by the size of the crystals studied; the difference probably results from the greater polarizability of Se as well as potential resonance effects.

Resistivity Studies. The three compounds measured, namely Ba_4USe_6, Ba_3FeUSe_6, and Ba_3MnUSe_6, are narrow gap semiconductors (Figure 5). Resistivity drops from 2.3 kΩ cm at 300 K to 0.66 kΩ cm at 500 K for Ba_4USe_6, from 85 Ω cm to 46 Ω cm for Ba_3FeUSe_6, and from 128 Ω cm to 99 Ω cm for Ba_3MnUSe_6. The activation energy extracted from the corresponding Arrhenius plots is 0.08(1), 0.04(1), and 0.02(1) eV for Ba_4USe_6, Ba_3FeUSe_6, and Ba_3MnUSe_6, respectively.

DFT Calculations. Four compounds were studied with density functional theory. The total (upper plot) and partial (lower plots) density of states of Ba_4USe_6, Ba_3FeUSe_6, Ba_3MnUSe_6, and Ba_3MnUS_6 are presented in Figures 6, 7, 8, and 9, respectively. They present some remarkable similarities in their electronic structure: all four compounds are found to be semiconducting with a band gap of 2.6 eV for Ba_4USe_6, 2.1 eV for Ba_3FeUSe_6, 1.8 eV for Ba_3MnUSe_6, and 2.1 eV Ba_3MnUS_6. The states just below the Fermi level (put at zero eV on the plots) are derived mainly from U-f states with some contribution from other atoms, mainly Fe-d and Mn-d states for the three compounds containing a transition metal. The U, Fe, and Mn atoms carry a magnetic moment, which is seen from the corresponding asymmetric partial density of states. These magnetic moments induce a small magnetic polarization on the other atoms (S, Se, and Ba), which is seen from their partial density of states.

CONCLUSIONS

The 2H hexagonal perovskite-related family exhibits remarkable chemical flexibility. We show that the 5f element U is very flexible with respect to its position within the structure and its oxidation state. The six new uranium chalcogenides, Ba_4USe_6, Ba_3FeUSe_6, Ba_3MnUSe_6, Ba_3MnUS_6, $Ba_{3.3}Rb_{0.7}US_6$, and $Ba_{3.2}K_{0.8}US_6$, represent an example of this flexibility. These compounds, synthesized by solid-state methods at 1173 K, are isostructural and crystallize in the K_4CdCl_6 structure type in space group D_{3d}^6−$R\bar{3}c$ of the trigonal system with six formula units per cell. In Ba_3FeUSe_6, Ba_3MnUSe_6, and Ba_3MnUS_6, the structure consists of infinite $^1_\infty[MUQ_6^{6-}]$ chains (M = Fe or Mn; Q = S or Se) oriented along the *c* axis that are separated by Ba atoms. These chains are composed of alternating M-centered octahedra and U-centered trigonal prisms sharing triangular faces; in contrast, in the structures of Ba_4USe_6, $Ba_{3.3}Rb_{0.7}US_6$, and $Ba_{3.2}K_{0.8}US_6$ U-centered octahedra alternate with Ba-, Rb-, or K-centered trigonal prisms along the *c* axis. Moreover, the Ba_4USe_6, Ba_3FeUSe_6, Ba_3MnUSe_6, and Ba_3MnUS_6 compounds contain U^{4+}, whereas $Ba_{3.3}Rb_{0.7}US_6$ and $Ba_{3.2}K_{0.8}US_6$ are mixed $U^{4+/5+}$ compounds. Moreover, *μ*-Raman spectroscopic measurements provide additional insight into these interesting subtle structural variations. Resistivity measurements show that Ba_4USe_6, Ba_3FeUSe_6, and Ba_3MnUSe_6 are semiconductors with activation energies of 0.08(1), 0.04(1), and 0.02(1) eV. Band gaps calculated using the HSE06 functional are 2.6, 2.1, and 1.8 eV, respectively, for these compounds and 2.1 eV for Ba_3MnUS_6.

ASSOCIATED CONTENT

Supporting Information

Crystallographic file in CIF format for Ba_4USe_6, Ba_3FeUSe_6, Ba_3MnUSe_6, Ba_3MnUS_6, $Ba_{3.3}Rb_{0.7}US_6$, and $Ba_{3.2}K_{0.8}US_6$. This material is available free of charge via the Internet at http://pubs.acs.org.

AUTHOR INFORMATION

Corresponding Author

*E-mail: ibers@chem.northwestern.edu.

Notes

The authors declare no competing financial interest.

ACKNOWLEDGMENTS

Use was made of the IMSERC X-ray Facility at Northwestern University, which is supported by the International Institute of Nanotechnology (IIN). S.L. acknowledges HPC resources from GENCI-CCRT/CINES (Grant x2014-085106). Optical measurements were supported by the National Science Foundation Grant CHE-1152547. C.D.M. was supported by the U.S. Department of Energy, Office of Basic Energy Sciences, under Contract DE-AC02-06CH11357. This material is based upon

DOI: 10.1021/ic5029806
Inorg. Chem. 2015, 54, 2851−2857

work supported by the National Science Foundation Graduate Research Fellowship under Grant DGE-1324585. Any opinions, findings, conclusions or recommendations expressed in this material are those of the authors and do not necessarily reflect the views of the National Science Foundation.

REFERENCES

(1) Cava, R. J. *Dalton Trans.* **2004**, 2979−2987.
(2) Mitchell, R. H. *Perovskites: Modern and Ancient*; Almaz Press Inc.: Thunder Bay, Canada, 2002.
(3) Zhao, Q.; Darriet, J.; Whangbo, M.-H.; Ye, L.; Stackhouse, C.; zur Loye, H.-C. *J. Am. Chem. Soc.* **2011**, *133*, 20981−20994.
(4) Stitzer, K. E.; Darriet, J.; zur Loye, H.-C. *Curr. Opin. Solid State Mater. Sci.* **2001**, *5*, 535−544.
(5) zur Loye, H.-C.; Zhao, Q.; Bugaris, D. E.; Chance, W. M. *CrystEngComm* **2012**, *14*, 23−39.
(6) Danielson, E.; Devenney, M.; Giaquinta, D. M.; Golden, J. H.; Haushalter, R. C.; McFarland, E. W.; Poojary, D. M.; Reaves, C. M.; Weinberg, W. H.; Di Wu, X. *Science* **1998**, *279*, 837−839.
(7) Wang, S.; Liu, Z.; Peters, J. A.; Sebastian, M.; Nguyen, S. L.; Malliakas, C. D.; Stoumpos, C. C.; Im, J.; Freeman, A. J.; Wessels, B. W.; Kanatzidis, M. G. *Cryst. Growth Des.* **2014**, *14*, 2401−2410.
(8) Hase, M.; Terasaki, I.; Uchinokura, K. *Phys. Rev. Lett.* **1993**, *40*, 3651−3654.
(9) Takahashi, J.; Shimada, M.; Yamane, H. *Phys. Status Solidi A* **2006**, *203*, 2836−2840.
(10) Aasland, S.; Fjellvag, H.; Hauback, B. *Solid State Commun.* **1997**, *101*, 187−192.
(11) Wu, H.; Haverkort, M. W.; Hu, Z.; Khomskii, D. I.; Tjeng, L. H. *Phys. Rev. Lett.* **2005**, *95*, 186401−186404.
(12) Mikami, M.; Funahashi, R.; Yoshimura, M.; Mori, Y.; Sasaki, T. *J. Appl. Phys.* **2003**, *94*, 6579−6582.
(13) Perez-Mato, J. M.; Zakhour-Nakhl, M.; Weill, F.; Darriet, J. *J. Mater. Chem.* **1999**, *9*, 2795−2808.
(14) Sun, Y.-Y.; Agiorgousis, M. L.; Zhang, P.; Zhang, S. *Nano Lett.* **2015**, *15*, 581−585.
(15) Yao, J.; Ibers, J. A. *Z. Anorg. Allg. Chem.* **2008**, *634*, 1645−1647.
(16) Beck, H. P.; Milius, W. *Z. Anorg. Allg. Chem.* **1986**, *539*, 7−17.
(17) Mesbah, A.; Ibers, J. A. *J. Solid State Chem.* **2013**, *199*, 253−257.
(18) Mesbah, A.; Malliakas, C. D.; Lebègue, S.; Sarjeant, A. A.; Stojko, W.; Koscielski, L. A.; Ibers, J. A. *Inorg. Chem.* **2014**, *53*, 2899−2903.
(19) Feng, K.; Shi, Y.; Yin, W.; Wang, W.; Yao, J.; Wu, Y. *Inorg. Chem.* **2012**, *51*, 11144−11149.
(20) Bugaris, D. E.; Ibers, J. A. *J. Solid State Chem.* **2008**, *181*, 3189−3193.
(21) Haneveld, A. J. K.; Jellinek, F. *J. Less-Common Met.* **1969**, *18*, 123−129.
(22) Noël, H. *Physica B+C* **1985**, *130*, 499−500.
(23) Mansuetto, M. F.; Jobic, S.; Ng, H. P.; Ibers, J. A. *Acta Crystallogr., Sect. C: Cryst. Struct. Commun.* **1993**, *49*, 1584−1585.
(24) Grey, I. E.; Steinfink, H. *Inorg. Chem.* **1971**, *10*, 691−696.
(25) *Bruker APEX2 Version 2009.5−1 Data Collection and Processing Software*; Bruker Analytical X-Ray Instruments, Inc.: Madison, WI, USA, 2009.
(26) Sheldrick, G. M. *SADABS; Department of Structural Chemistry*; University of Göttingen: Göttingen, Germany, 2008.
(27) Sheldrick, G. M. *Acta Crystallogr., Sect. A: Found. Crystallogr.* **2008**, *64*, 112−122.
(28) Gelato, L. M.; Parthé, E. *J. Appl. Crystallogr.* **1987**, *20*, 139−143.
(29) Spek, A. L. PLATON, A. *Multipurpose Crystallographic Tool*; Utrecht University, Utrecht: The Netherlands, 2014.
(30) Holland, M.; Donakowski, M. D.; Pozzi, E. A.; Rasmussen, A. M.; Thao Tran, T.; Pease-Dodson, S. E.; Halasyamani, S.; Seideman, T.; Van Duyne, R. P.; Poeppelmeier, K. R. *Inorg. Chem.* **2014**, *53*, 221−228.
(31) Kresse, G.; Forthmüller, J. *Comput. Mater. Sci.* **1996**, *6*, 15−50.
(32) Kresse, G.; Joubert, D. *Phys. Rev. B* **1999**, *59*, 1758−1775.
(33) Heyd, J.; Scuseria, G. E.; Ernzerhof, M. *J. Chem. Phys.* **2003**, *118*, 8207−8215.
(34) Heyd, J.; Scuseria, G. E.; Ernzerhot, M. *J. Chem. Phys.* **2006**, *124*, 219906-1.
(35) Paier, J.; Marsman, M.; Hummer, K.; Kresse, G.; Gerber, I. C.; Angyan, J. G. *J. Chem. Phys.* **2006**, *124*, 154709.
(36) Paier, J.; Marsman, M.; Hummer, K.; Kresse, G.; Gerber, I. C.; Angyan, J. G. *J. Chem. Phys.* **2006**, *125*, 249901-1−249901-2.
(37) Kohn, W.; Sham, L. J. *Phys. Rev.* **1965**, *140*, 1133−1138.
(38) Hohenberg, P.; Kohn, W. *Phys. Rev.* **1964**, *136*, 864−871.
(39) Blöchl, P. E. *Phys. Rev. B* **1994**, *50*, 17953−17979.
(40) Ward, M. D.; Ibers, J. A. *Z. Anorg. Allg. Chem.* **2014**, *640*, 1585−1588.
(41) Mesbah, A.; Stojko, W.; Malliakas, C. D.; Lebegue, S.; Clavier, N.; Ibers, J. A. *Inorg. Chem.* **2013**, *52*, 12057−12063.
(42) Lu, Y.-J.; Ibers, J. A. *Comments Inorg. Chem.* **1993**, *14*, 229−243.
(43) Oh, G. N.; Choi, E. S.; Ibers, J. A. *Inorg. Chem.* **2012**, *51*, 4224−4230.
(44) Bugaris, D. E.; Ibers, J. A. *J. Solid State Chem.* **2009**, *182*, 2587−2590.
(45) Jin, G. B.; Ringe, E.; Long, G. J.; Grandjean, F.; Sougrati, M. T.; Choi, E. S.; Wells, D. M.; Balasubramanian, M.; Ibers, J. A. *Inorg. Chem.* **2010**, *49*, 10455−10467.
(46) Deiseroth, H.-J.; Aleksandrov, K.; Kremer, K. K. *Z. Anorg. Allg. Chem.* **2005**, *631*, 448−450.
(47) Wintenberger, M.; Jumas, J. C. *Acta Crystallogr.* **1980**, *B36*, 1993−1996.
(48) Ward, M. D.; Klingsporn, J. M.; Ibers, J. A. *Inorg. Chem.* **2013**, *52*, 10220−10222.
(49) Badger, R. M. *J. Chem. Phys.* **1934**, *2*, 128−131.

DOI: 10.1021/ic5029806
Inorg. Chem. 2015, 54, 2851−2857